

Chapter 4

Climate Change and Hydrological Responses in Himalayan Basins, Nepal

Tirtha Raj Adhikari and Lochan Prasad Devkota

Abstract Studies on water and related fields are vital for protecting the environment and climate. Lack of hydrometeorological data, particularly in a high-altitude region such as Nepal, hinders the process of understanding the systems of earth science dynamics. In this study, observed data were used for the period 1988–2010 from three high-altitude regions, viz., Annapurna, Langtang, and Khumbu, of Nepal. The Coupled Global Climate Model (CGCM3) for A1B SRES scenarios during the period 2001–2060 was used to determine projections. The statistical downscaling model (SDSM) was used to downscale precipitation and temperature data at the Modi, Langtang, and Dudh Koshi river basins. The simulated precipitation and temperature data were corrected for bias before implementation in the conceptual rainfall–runoff model Hydraologiska Byrans Vattenbalansavde (HBV) for hydrological response analysis. In the HVB-light 3.0, the Groups Algorithms Programming (GAP) optimization approach and calibration were used to obtain several parameter sets that were ultimately reproduced to observe the stream flow.

The CGCM3 model projects increasing trends in annual as well as seasonal precipitation, except in summer [June, July August, September (JJAS)], during 2001–2060 for A1B SERS emission scenarios over the three sites under investigation. The model projects warmer days in every season of the entire period from 2001 to 2060. These warming trends are higher in maximum than in minimum temperatures throughout the year, which indicates an increasing trend of daily temperature range as the greenhouse effect increases. Further, trends for post-monsoon (ON) temperature are much cooler compared to the remaining three seasons (months) over all three sites. In addition, decreasing trends in summer discharge at Langtang Khola and increasing trends in Modi Khola and Dudh Koshi river basins are evident. Among all basins, the flow regime is more pronounced during the later parts of future decades as compared to the preceding decades.

Keywords Temperature • Precipitation and discharge trends • SDSM • HVB-light 3.0 • Bias correction

T.R. Adhikari (✉) • L.P. Devkota
Central Department of Hydrology and Meteorology, Tribhuvan University,
Kirtipur, Kathmandu, Nepal
e-mail: tirtha43@yahoo.com

4.1 Introduction

This research focuses on a comparative study of the impact of climate change on the flow regime in three perennial monsoon-dominated river basins of Nepal Himalaya. The Statistical Downscaling Model (SDSM), version 4.2.2, and HVB-light 3.0 software have been used for climate and river runoff simulation. The SDSM is a hybrid of a regression method and weather generator; mainly statistical downscaling methods have not been documented for the climate research in these river basins of Nepal (Rashid and Mukand 2012), so research based on SDSM and HVB-light 3.0 is at an early stage. The main objectives of this chapter are to evaluate the application of SDSM over these three basins in Nepal and to generate local-scale precipitation and temperature scenarios under future emission scenarios. The HVB-light 3.0 hydrological model, which is a conceptual hydrological model for continuous simulation of runoff, is used for discharge simulations in all three basins. This HVB model was originally developed at the Swedish Meteorological and Hydrological Institute (SMHI) in the early 1970s to assist hydropower operations (Bergstrom and Graham 1998) by providing hydrological forecasts. The HVB-light 3.0 model simulates daily discharge using daily rainfall and temperature data and monthly estimates of potential evaporation. In this study, basin-wise temperature and precipitation have been simulated on the basis of observed data for the climate change scenario, and these values have been used as input for the hydrological model HVB-light 3.0. In recent years, numerous studies have investigated the impact of climate change on hydrology and hydrological responses in many regions. Charlton et al. (2006) investigated the impact of climate change on water supplies and flood hazard in Ireland using a grid-based approach, the HYSIM model (Manley 1993), with statistically downscaled climate data from the Hadley Centre Climate Model, HadCM3 (Gordon et al. 2000). Murphy et al. (2006a) employed similar downscaled data to force the HYSIM model, modeling individual basins rather than a gridded domain. A regional climate model is used to produce the dynamically downscaled precipitation and temperature data that are required by the HVB-light 3.0 conceptual rainfall–runoff model.

The effects of global warming on the glaciers and ice reserves of Nepal has serious implications for freshwater reserves and consequently for low flows. Any significant change in glacier mass and groundwater storage will impact the water resource at a regional scale. Increases in temperature and precipitation in the Himalayas accelerate the melting of ice and snow as well as enhancing flooding events from direct runoff, whereas the dry season discharge (base flow) decreases. The projected changes in climatic parameters have an adverse effect on the water storage capacity of the Nepal Himalaya. The major concerns are the rapid reduction of glaciers in much of the Himalayan region and the upward shift of the snow line.

In the past, many attempts have been made to study climate change impact and hydrological responses. Most of these studies have focused on extreme events such as flood and drought, whereas climate change studies in Himalayan regions have

focused mainly on the melting and retreating of glaciers, glacial lake outburst floods (GLOF), and their trends. In this study, however, the temperature, precipitation, and discharge trends of three basins are presented.

4.2 Study Area

Nepal is situated in the middle of the Hindu Kush Himalayan region. The country extends between 26°22' and 30°27' N latitude and 80°40' and 88°12' E longitude; it is surrounded by India to the east, south, and west and China to the north. The country is about 885 km in length from east to west, and the north–south width varies from 145 to 241 km. Within this range, the altitudinal variations are from about 60 m above mean sea level (a.m.s.l.) in the southern plain (called Terai) to Mount Everest (8848 m) in the northeast. Of the total area of the country, 147,181 km², about 86 % of the area is composed of hilly and mountainous regions and the remaining 14 % of flatlands.

In general, the country is divided into five major physiographic zones: the Terai, Siwalik, Hill, middle mountain, and high mountain. The Terai is characterized by a long narrow belt of fertile agricultural flatland; it is part of the alluvial Gangetic Plains and ranges in altitude from 60 to 300 m. It lies between the Indian border in the south and the first outer foothills of Nepal in the north. The Siwalik range, 600–1500 m in elevation, lies in the north of the Terai region. To the north of Siwalik is a zone of discontinuous valleys (also called “Dun”). Intensive cultivation and decreasing forest cover have been causing serious problems of soil erosion in these valleys. Further north of these valleys is the Mahabharat Range (2700–3700 m), which, in terms of formation and elevation, is well developed in eastern and central Nepal and poorly developed in western Nepal. The northernmost part of Nepal is the snowy mountainous region (Himalaya), which is above 4000 m in elevation and stretches from the east to the west of the country.

This research focuses only on the impact of climate change on hydrological responses within three perennial monsoon-dominated river basins of Nepal's Himalayan region. The basins studied are the Modi Khola river basin in Annapurna region, the Langtang Khola river basin in Langtang region, and the Dudh Koshi river basin in Khumbu region.

Three watersheds—Modi Khola river basin (Annapurna), Langtang Khola river basin (Langtang), and Dudh Koshi river basin (Khumbu)—with areas of 640.79 km², 583.41 km², and 3710.30 km², respectively, were selected for this study. The Modi Khola river basin hydrological station is situated at latitude 28.12° N and longitude 83.42° E, and the meteorological station is situated at latitude 28.13°–28.31° N and longitude 83.42°–83.57° E. Its elevation ranges between 667 and 8024 m a.m.s.l. Similarly, the Syabrubesi hydrological station is located at latitude 28.16° N and

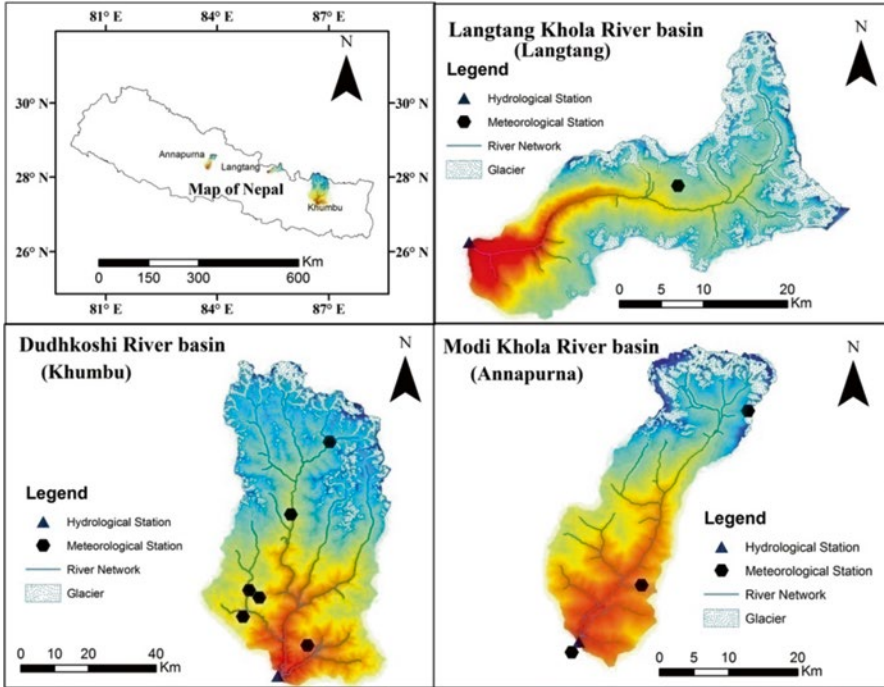


Fig. 4.1 Location of Langtang Khola, Dudh Koshi, and Modi Khola river basins in Nepal (Source: Author)

longitude 85.35° E and the Langtang Kyanging meteorological station at latitude 28.22° N and longitude 85.62° E. The elevation ranges from 1434 amsl up to the peak of Langtang Lirung at 7234 amsl. The Rabuwa Bazar hydrological station is found at latitude 27.16° N and longitude 86.65° E and the Khumbu region meteorological stations at latitude 27.21° – 27.89° N and longitude 86.45° – 86.83° E, where the elevation ranges from 439 to 8848 amsl. The location of each river basin in Nepal is presented in Fig. 4.1.

4.2.1 Watershed Characteristics of the Three Basins

Watershed characteristics depend upon peak discharge, time variation of runoff (hydrography), stage versus discharge, total volume of runoff, and frequency of runoff (statistics and return period). However, in this study, the flow regime of all three river basins is dependent on monsoon storms and the glacier area and its contribution to melting. In Nepal, the flow regime is divided into seven drainage basins:

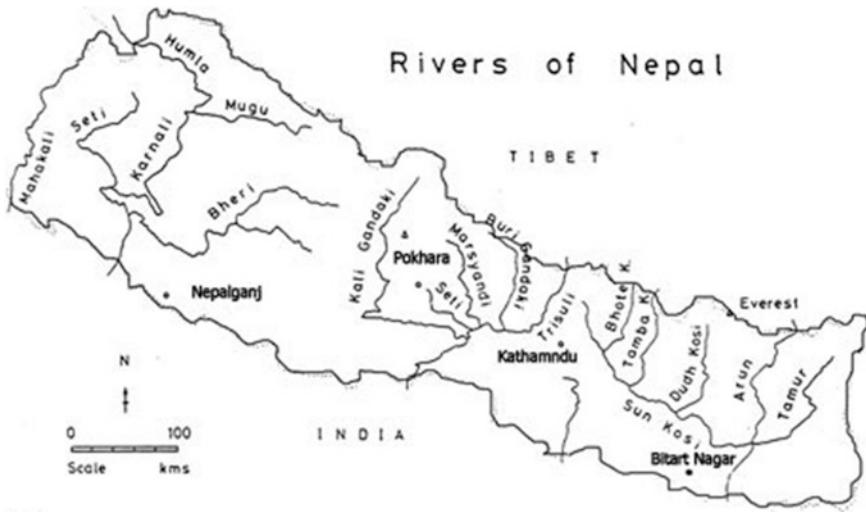


Fig. 4.2 The major river systems of Nepal (Source: Author)

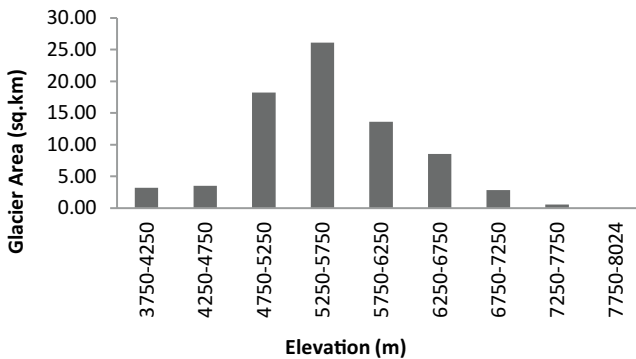


Fig. 4.3 Glacier area and elevation characteristics of Modi Khola river basin (Source: Author)

the Kankai Mai river basin, the Koshi river basin, the Bagmati river basin, the Narayani river basin, the West Rapti river basin, the Karnali river basin, and the Mahakali river basin (Fig. 4.2).

Among these, only three sub-river basins, that is, the Modi Khola, Langtang Khola, and Dudh Koshi river basins, were considered for this study. In the Modi Khola river basin, the highest glacier area was found between 2550 and 5750 m (Fig. 4.3) and in the Langtang Khola river basin between 5434 and 5934 m (Fig. 4.4). The Dudh Koshi river basin has the greatest glacier area, 413.2 km², between 4500 and 5000 m in elevation (Fig. 4.5).

Fig. 4.4 Glacier area and elevation characteristics of Langtang Khola river basin (Source: Author)

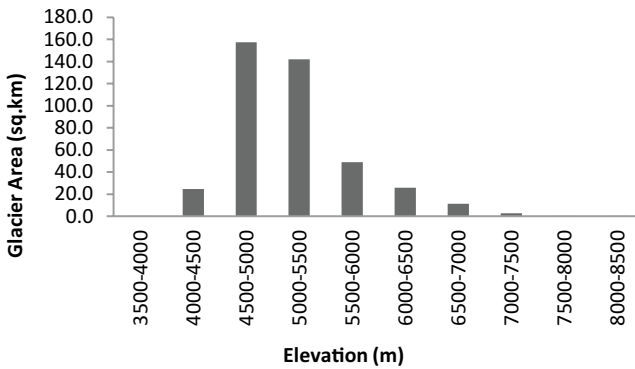
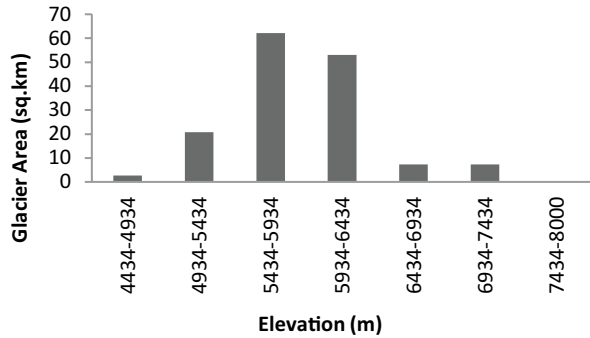


Fig. 4.5 Glacier area and elevation characteristics of Dudh Koshi river basin (Source: Author)

4.3 Data Collection and Quality Control

All necessary temperature, precipitation, and discharge data are collected for different periods from the Department of Hydrology and Meteorology (DHM), Government of Nepal (Table 4.1). The collected observed meteorological data from 1988 to 2010 and the observed discharge data from 1991 to 2010 were used for model calibration and validation purposes.

The time-series data are considered to be acceptable only if they satisfy the homogeneity and consistency of quality control (WMO 1988). Sen’s slope method was used to check the quality of the available data. Annual meteorological data were shown as blank if there were missing values in the series for any period, because Sen’s slope estimation method allows estimating trend with missing values. The double mass analysis (sometimes called double sum analysis) is a useful method for assessing homogeneity in a weather parameter (Allen et al. 1998; Raghunath 2006; Silveira 1997). It is a useful tool for checking the consistency of a climatic variable

Table 4.1 Characteristics of hydroclimatic data collected from Department of Hydrology and Meteorology (DMH), Government of Nepal

Station name	Type	Latitude (N)	Longitude (E)	Elevation (m)	Record period	Missing period
Machhapuchhre ^a	Climatic	28.31	83.57	3470	1987–2010	1996 and 1997
Lumle ^a	Climatic	28.18	83.48	1740	1969–2010	No
Parbat ^a	Precipitation	28.13	83.42	891	1969–2010	1969 (Jan–May)
Modi ^b	Hydrological	28.12	83.42	667	1991–2010	No
Langtang ^a	Climatic	28.22	85.62	3920	1987–2010	No
Sabrubasi ^b	Hydrological	28.16	85.35	1434	1991–2010	No
Dingboche Khumbu ^a	Climatic	27.89	86.83	4355	1987–2010	2000, 2001 and 2002
Chaurikhark ^a	Precipitation	27.42	86.43	2619	1949–2010	1952
Parkarns ^a	Precipitation	27.26	86.34	1982	1948–2010	No
Aiselukhark ^a	Precipitation	27.21	86.45	2143	1948–2010	No
Okhaldhunga ^a	Climatic	27.32	86.50	1720	1948–2010	1958
Mane Bhanjyang ^a	Precipitation	27.29	86.25	1576	1948–2010	No
Salleri ^a	Precipitation	27.3	86.35	2378	1948–2010	1962 – 1972
Dudh Koshi Rabuwa ^b	Hydrological	27.16	86.65	460	1964–2010	No

^aMeteorological station^bHydrological station

where the error results from such reasons as a change in the environment (or exposure) of a station, for example, planting trees or cutting nearby forest, which affects the catch of the gauge because of differences in wind pattern or exposure. Replacement of the recording instruments with a new system might also result in such deviations (Raghunath 2006).

4.4 Methodology

Analysis of the effects of climate change on hydrological responses in Modi Khola river basin (Annapurna region), Langtang Khola river basin (Langtang region), and Dudh Koshi river basin (Khumbu region) was selected for this study. Selections were made on the basis of the availability of relatively better hydrometeorological data compared to other regions of the Nepal Himalayas. The following methodology was applied in this study.

- Downloading SRTM DEM data (<http://www.cgiar-csi.org/data/srtm-90m-digital-elevation-database-v4-1>) and separation of the study basin were done by GIS software. The SRTM digital elevation data, produced by NASA originally, are a major breakthrough in digital mapping of the world and provide a major advance in accessibility of high-quality elevation data for large portions of the tropics and other areas of the developing world.
- Collection of daily hydrometeorological data and evaluation of data quality included classification into seasons: winter, December of the previous year to February (DJF); spring, March to May (MAM); summer, June to September (JJAS); and autumn, October to November (ON).
- Calibration of SDSM and validation of the SDSM model followed the generation of a temperature and rainfall scenario by SDSM. The generated rainfall and temperature data are compared with observed and modeled data for bias correction.
- The biased rainfall and temperature data have been corrected and were used later in the hydrological model for the generation of the discharge scenario. These generated scenario data were computed for generating the seasonal trends.
- Comparison of the seasonal trend of all three basins.

4.4.1 Bias Correction Methodology

Results from GCMs and regional climate models (RCMs) always show some degree of bias for both temperature and precipitation data. The reasons for such biases include systematic model errors caused by imperfect conceptualization, discretization, and spatial averaging within the grids. The bias correction approach is used to eliminate the biases from the daily time-series of downscaled data (Salzmann et al. 2007). In this study, Eqs. 4.1 and 4.2 are used to de-bias daily temperature and precipitation data (Mahmood and Mukand 2012):

$$T_{\text{deb}} = T_{\text{SCEN}} - (\bar{T}_{\text{CONT}} - \bar{T}_{\text{obs}}) \quad (4.1)$$

$$P_{\text{deb}} = P_{\text{SCEN}} \times \left(\frac{\bar{P}_{\text{obs}}}{\bar{P}_{\text{CONT}}} \right) \quad (4.2)$$

where T_{deb} and P_{deb} are bias-corrected daily temperature and precipitation, respectively; T_{SCEN} and P_{SCEN} are daily temperature and precipitation, respectively, obtained from downscale data (SDSM); \bar{T}_{obs} and \bar{P}_{obs} are long-term monthly mean of observed temperature and precipitation, respectively; and \bar{T}_{CONT} and \bar{P}_{CONT} are long-term monthly mean of temperature and precipitation, respectively, simulated using SDSM for the observed period.

In Sen's method, if a linear trend is present in a time-series, then the true slope (change per unit time) can be estimated by using a simple nonparametric procedure developed by Sen (1968); thus, in the linear model $f(t)$ can be described as

$$f(t) = Qt + B \quad (4.3)$$

where Q is the slope and B is a constant. To derive an estimate of the slope Q , the slopes of all data pairs are calculated:

$$Q_i = \frac{Z_j - Z_k}{(j - k)} \text{ where } j > k \quad (4.4)$$

If there are n values of Z_j in the time-series, we obtain as many as $N = n(n-1)/2$ slope estimates of Q_i . Sen's estimator of slope is the median of these N values of Q_i . The N values of Q_i are ranked from the smallest to the largest, and Sen's estimator is

$$Q = \left\{ \begin{array}{l} \frac{Q_{N+1}}{2} \text{ if } N \text{ is odd} \\ \frac{1}{2} \left\{ Q_{\frac{N}{2}} + Q_{\frac{N+2}{2}} \right\} \text{ if } N \text{ is even} \end{array} \right\} \quad (4.5)$$

The foregoing equations were used for the Mann-Kendall test and Sen's slope estimation in this study. The normal variate statistics (Z) and Sen's slope were obtained from the calculation for each month and also for the annual time-series. The presence of a statistical significance of trend was evaluated using the Z value.

To test for either an upward or downward monotone trend (a one-tailed test) at the α -level of significance, H_0 (no trend) was rejected if the absolute value of Z is greater than $Z_{1-\alpha}$ where $Z_{1-\alpha}$ was obtained from the standard normal cumulative distribution tables. The significance level of 0.05 means that there is a 5 % probability that the values of Z_i are from a random distribution, and with that probability we are in error when rejecting H_0 of no trend. Sen's slope is available as average change per year; a negative value indicates a negative trend and a positive value indicates a positive trend.

4.4.2 *HVB-Light 3.0 Methodology for Model Calibration and Validation*

The present study builds on the work of Wang (2006) to develop a methodology that is used with an ensemble of dynamically downscaled climate data to investigate the impacts of climate change on the hydrology of Irish rivers. Wang (2006) used the HBV model (Bergstrom 1992) from the Swedish Meteorological and Hydrological Institute (SMHI), which is usually calibrated using a manual trial-and-error approach. Here, it has been replaced by the *HVB-light 3.0* model of Seibert (2005) because its interface allows Monte Carlo simulations. Calibration using the Monte Carlo method yields an ensemble of simulations that allows accounting for parameter uncertainty in analysis. A Monte Carlo approach to calibration was used in which the 99th percentile of an ensemble of 10,000 parameter sets was selected for use in the impact study. This approach allows the inclusion of an uncertainty parameter in the study, which provides a range of possible values, rather than a single value, that further allows an estimation of confidence in the research outcome. The *HVB-light 3.0* model was validated for a reference period (1961–2000) to ensure that stream flow was modeled correctly. A persistent positive bias in the downscaled precipitation was observed and removed to improve the agreement between modeled and observed stream flow. It was shown that the impact of parameter uncertainty on the validation of seasonal (winter and summer) flow was less significant than in the annual maximum daily mean flow. To investigate the hydrological and catchment characteristics, analysis of the affecting parameter was carried out, the missing dataset of temperature and precipitation was filled by the statistical downscaling model, and the conceptual model was run several times to generate three different results by varying the parameter affecting the hydrological characteristics. Three sets of methods including one without using a glacier component and another using the glacier component were derived, and finally simulation of river discharge by the *HVB-light 3.0* model was carried out by assuming the temperature increase. Konz and Merz (2010) applied the HBV model for the Tamor River to estimate runoff at Tapethok, Taplejung, in eastern Nepal. In general, the HBV model was able to correctly simulate low flow, except for some sharp peaks caused by isolated precipitation events (Konz and Merz 2010). In this study, a similar analysis was carried out, and similar results were obtained because the HBV model was able to simulate low flows very well, with the exception of sharp peaks. The model *HVB-light 3.0* was calibrated for the three river basins, and basin areas were divided into 15 elevation zones in the Modi Khola river basin, into 13 elevation zones in the Langtang river basin, and into 17 elevation zones in Dudh Koshi river basin. Two vegetation zone, namely, the glacier and the vegetated area for the calibration period, were used, and the *HVB-light 3.0* model was calibrated by trial-and-error technique in the study of the three basins.

4.5 Results

4.5.1 Observed Maximum Temperature

The observed seasonal maximum temperature is approximately 13.2 °C in spring at Annapurna, and similarly the observed seasonal minimum temperature is around -8.0 °C during winter at Khumbu, whereas the observed seasonal mean annual temperature is about 3.3 °C at Annapurna and Khumbu, for all seasons (Tables 4.2, 4.3, 4.4).

Table 4.2 Observed seasonal maximum temperature (°C) (1988–2010)

Season ^a	Annapurna	Langtang	Khumbu
DJF	4.4	3.6	3.5
MAM	11.6	7.8	11.0
JJAS	13.2	11.7	10.1
ON	6.3	5.0	5.2
Annual	13.2	11.7	11.0

^a*DJF* December January February, *MAM* March April May, *JJAS* June July August September, *ON* October November

Table 4.3 Observed minimum temperature (°C) (1988–2010)

Season	Annapurna	Langtang	Khumbu
DJF	-4.3	-6.3	-8.0
MAM	1.4	-1.1	-1.2
JJAS	6.7	6.2	2.9
ON	0.4	-0.8	-1.6
Annual	-4.3	-6.3	-8.0

Table 4.4 Observed seasonal mean annual temperature (°C) (1988–2010)

Season	Annapurna	Langtang	Khumbu
DJF	-1.9	-1.3	-3.4
MAM	4.9	3.4	3.7
JJAS	8.1	8.9	6.2
ON	2.2	2.1	1.3
Annual	3.3	3.3	2.0

4.5.2 Observed Annual Temperature Trend

Observed seasonal maximum temperature trends for 1988–2010 are depicted in Table 4.5. All three regions show the highest maximum and mean temperature, with an increasing trend, in winter (DJF). The lowest minimum temperature trends are found to occur during spring (MAM) in Annapurna and summer (JJAS) in the Khumbu regions. Similarly, the highest annual maximum temperature trend, of 0.1414 °C/year, is found in the Langtang region among the three regions, and the lowest minimum temperature trend observed was –0.0024 °C/year in the Khumbu region.

4.5.3 Observed Precipitation Distribution

The month of July has the highest rainfall, followed by August, in the Modi Khola and the Dudh Koshi river basins. The monsoon precipitation is more pronounced in the Modi Khola and Dudh Koshi river basins. In the Langtang Khola river basin, the month of August yields the highest rainfall, followed by July. The total precipitation in the Modi Khola river basin during the summer (JJAS) is 2062 mm, of which 85 % of the rainfall occurs in the monsoon season, and rainfall of 44 mm occurs during winter (DJF). Similarly, the total precipitation of Langtang Khola river basin during the summer (JJAS) is 492 mm, of which 78 % of the precipitation occurs in the monsoon season, with precipitation of 20 mm during the autumn (ON) season. The total precipitation for the Dudh Koshi river basin during the summer (JJAS) is 345 mm, of which 80 % of precipitation occurs in the monsoon season, with precipitation of 9 mm in winter (DJF) (Table 4.6). The maximum coefficient of variation was exceeded in November at the Modi Khola river basin (Fig. 4.6) and the Dudh Koshi river basin (Fig. 4.7). Similarly, the coefficient of variation was exceeded in October at the Langtang Khola river basin (Fig. 4.8).

4.5.4 Observed Precipitation Trends

The observed highest precipitation trend of 2.2249 mm/year was found during winter (DJF) in the Langtang region (Table 4.7). The lowest precipitation trend, –0.3386 mm/year, occurs in the Khumbu region in summer (JJAS). Similarly, observed annual precipitation trends are found to increase at a rate of 2.7452 mm/year in the Annapurna region. The observed annual precipitation trend has been found to be decreasing at the rate of –0.8264 mm/year in the Khumbu region.

Table 4.5 Observed temperature trends of the three river basins (1988–2010)

Season	Maximum			Minimum			Mean		
	Annapurna	Langtang	Khumbu	Annapurna	Langtang	Khumbu	Annapurna	Langtang	Khumbu
DJF	0.1129	0.1852	0.0857	0.0242	0.1267	0.0108	0.0657	0.1529	0.0857
MAM	0.0956	0.1718	0.0628	-0.0438	0.1115	0.0101	0.031	0.1421	0.0628
JJAS	0.081	0.1182	0.0499	0.0135	0.049	-0.0024	0.047	0.0838	0.0499
ON	0.0878	0.0992	0.0495	0.0021	0.0857	0.0045	0.0421	0.0924	0.0495
Annual	0.0955	0.1414	0.0639	0.0002	0.0884	0.0036	0.0499	0.0098	0.0639

Table 4.6 Observed precipitation distribution of the three river basins (1988–2010)

Seasons	Annapurna		Langtang		Khumbu	
	Seasonal total (mm)	Seasonal %	Seasonal total (mm)	Seasonal %	Seasonal total (mm)	Seasonal %
DJF	44	2	28	4	9	2
MAM	220	9	94	15	57	13
JJAS	2062	85	492	78	345	80
ON	109	4	20	3	20	5
Annual	2436	100	634	100	431	100

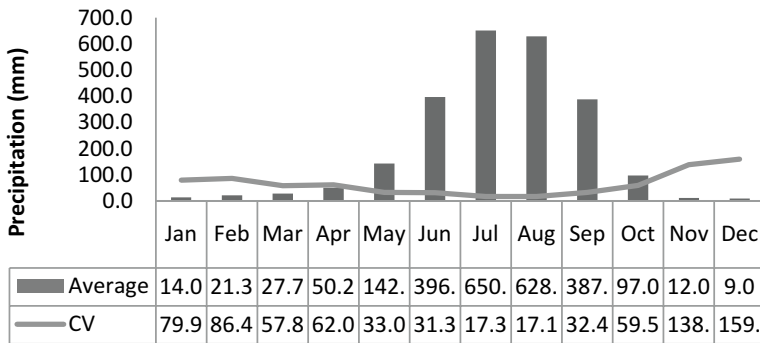


Fig. 4.6 Precipitation distribution of Modi Khola river basin (Source: Author)

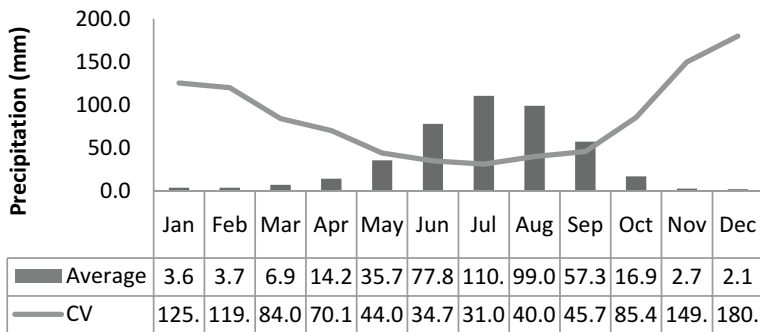


Fig. 4.7 Precipitation distribution of Dudh Koshi river basin (Source: Author)

4.5.5 Observed Discharge Distribution of the Three River Basins

The maximum discharge observed in the Annapurna region is 76 % in the Modi Khola basin, in the Langtang region, 57 % in the Langtang Khola basin, and in the Khumbu region, 77 % of the discharge, in the Dudh Koshi basin, is obtained in the summer season because of the monsoonal effect (Table 4.8).

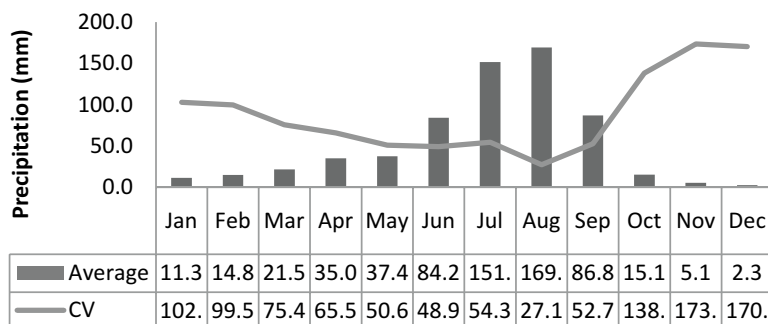


Fig. 4.8 Precipitation distribution of Langtang Khola river basin (Source: Author)

Table 4.7 Observed annual and seasonal precipitation trends of the three basins (1988–2010)

Season	Annapurna	Langtang	Khumbu
DJF	-0.6227	-0.2995	-0.0508
MAM	0.1094	0.2846	0.1320
JJAS	0.4398	2.2249	-0.3386
ON	1.3555	0.7979	0.1598
Annual	2.7452	10.608	-0.8264

Table 4.8 Seasonal observed discharge distribution (m^3/s) (1991–2010)

Season	Annapurna		Langtang		Khumbu	
	Seasonal total	Seasonal %	Seasonal total	Seasonal %	Seasonal total	Seasonal %
DJF	41	7	51	14	142	6
MAM	46	7	56	15	148	6
JJAS	468	76	212	57	1846	77
ON	62	10	51	14	276	11
Annual	617	100	369	100	2413	100

4.5.6 Observed Discharge and Trends of Three Basins

The annual trends of $-0.2984 \text{ m}^3/\text{s}$ and $-0.3799 \text{ m}^3/\text{s}$ are of decreasing order in Annapurna and Langtang regions, whereas the trend of $2.3072 \text{ m}^3/\text{s}$ is of increasing order in the Khumbu region (Table 4.9).

Table 4.9 Observed discharge and trends of the three basins (1991–2010)

Season	Annapurna		Langtang		Khumbu	
	1991–2000	2001–2010	1991–2000	2001–2010	1991–2000	2001–2010
DJF (m ³ /s)	11.1	15.8	17.5	16.5	43.1	47.9
MAM (m ³ /s)	13.7	17.3	19.6	17.8	48.1	46.4
JJAS (m ³ /s)	129.3	101.6	58.4	49.3	432	525.9
ON (m ³ /s)	66	57.8	54.9	47.7	267.2	247.5
Annual (m ³ /s)	54.9	47.1	33.4	28.9	189.2	219.8
Annual trend (1991–2010)	-0.2984		-0.3799		2.3072	

Table 4.10 Projected seasonal maximum temperature trend of A1B scenarios

Season	Maximum temperature (2001–2030)			Maximum temperature (2031–2060)		
	Annapurna	Langtang	Khumbu	Annapurna	Langtang	Khumbu
DJF	0.0183	0.0147	0.0216	0.0222	0.0071	0.0131
MAM	0.0285	0.0043	0.0294	0.0413	0.0037	0.0350
JJAS	0.0080	0.0160	0.0038	0.0159	0.0160	-0.0019
ON	0.0120	0.0085	-0.0102	-0.0059	-0.0012	-0.0032
Annual	0.0122	0.0144	0.0123	0.0203	0.0075	0.0116

Table 4.11 Projected seasonal minimum temperature trend of A1B scenarios

Season	Minimum temperature (2001–2030)			Minimum temperature (2031–2060)		
	Annapurna	Langtang	Khumbu	Annapurna	Langtang	Khumbu
DJF	0.0170	0.0366	-0.0039	0.0214	0.0249	-0.0013
MAM	0.0410	0.0414	0.0162	0.0517	0.0522	0.0043
JJAS	0.0102	0.0172	0.0241	0.0036	0.0139	0.0303
ON	-0.0650	0.0268	-0.0170	-0.0084	0.0278	0.0062
Annual	0.0151	0.0294	0.0085	0.0188	0.0300	0.0119

4.5.7 Projected Temperature Trends

The CGCM3-projected seasonal maximum temperature trend of A1B scenarios (Table 4.10) shows the highest maximum temperature with increasing trend in spring (MAM), except in Langtang (2001–2030), among all three regions. The lowest maximum temperature trend will occur in autumn (ON) among all three regions (2031–2060). Similarly, the highest annual maximum temperature trend, of 0.0203 °C/year, is found in the Annapurna region (2031–2060).

The CGCM3-projected seasonal minimum temperature trend of A1B scenarios is shown in Table 4.11. Lowest minimum temperature trends are found to occur in autumn (ON) in all regions except the Langtang region. The minimum temperature trends are found to increase during spring (MAM) in Annapurna and Langtang,

Table 4.12 Seasonal precipitation trend of A1B scenarios

Season	Precipitation trend of A1B (CGCM3: 2001–2030)			Precipitation trend of A1B (CGCM3: 2031–2060)		
	Annapurna	Langtang	Khumbu	Annapurna	Langtang	Khumbu
DJF	-0.0919	0.0174	0.0158	-0.1544	-0.00400	0.00070
MAM	-0.2728	0.0728	0.4109	0.55800	0.2220	0.2196
JJAS	-0.1327	0.0949	0.2420	0.02250	-0.1462	-0.2755
ON	-0.489	0.0072	-0.1277	2.7913	0.05850	-0.20770
Annual	2.9232	0.7621	1.9991	1.4753	0.20840	-0.8604

except in Khumbu (2031–2060). However, the lowest minimum temperature trends will occur in different seasons (2031–2060). Similarly, the highest annual minimum temperature trend, 0.0300 °C/year, is found to be increasing in Langtang compared to Khumbu and Annapurna regions during both projected periods.

4.5.8 Projected Precipitation Trends

The seasonal precipitation trends of the A1B scenarios is depicted in Table 4.12 (CGCM3: 2001–2060). In the Annapurna region, the precipitation trends are decreasing in all seasons, and the lowest precipitation occurs in autumn (ON), comparing all three regions (2001–2030), whereas the highest precipitation trends are found to occur in different seasons. Similarly, the highest precipitation trend, 2.7913 mm/year, is found to occur during autumn (ON) in Annapurna compared to Langtang and Khumbu (2031–2060). The lowest precipitation trend, -0.2755 mm/year, is found in the Khumbu region in summer (JJAS). Similarly, annual precipitation trends are increasing at the rate of 2.9232 mm/year and 1.4753 mm/year in Annapurna region (2001–2030 and 2031–2060, respectively), whereas in the Khumbu region, the annual precipitation trend has been found to be decreasing at -0.8604 mm/year (2001–2060). The annual precipitation trends of 0.7621 mm/year and 0.20840 mm/year are found in the Langtang region.

4.5.9 Projected Discharge Trends

The CGCM3-projected seasonal maximum discharge trend of A1B scenarios over the period of 2001–2060 is presented in Table 4.13. The maximum discharge in both Annapurna and Khumbu regions is found to be increasing in summer (JJAS), except in the Langtang region (2001–2030). Similarly, maximum discharge trends occur in different seasons (2031–2060). The lowest maximum discharge trend is found to occur during summer (JJAS) in the Langtang region (2001–2030) and during autumn (ON) in the Khumbu region (2031–2060). Similarly, annual maximum

Table 4.13 Projected seasonal maximum discharge trends of A1B scenarios

Season	Maximum (2001–2030)			Maximum (2031–2060)		
	Annapurna	Langtang	Khumbu	Annapurna	Langtang	Khumbu
DJF	0.0054	0.0479	0.2841	0.0135	0.0365	−0.0291
MAM	0.0788	0.0611	0.6692	0.0943	−0.0195	0.3399
JJAS	0.1315	−0.1010	1.7764	0.2535	0.0101	0.0984
ON	0.0693	0.1198	0.4291	0.0566	0.1408	−0.5431
Annual	0.0833	0.0277	0.7282	0.1208	0.0315	0.0193

Table 4.14 Projected seasonal minimum discharge trends of A1B scenarios

Season	Minimum (2001–2030)			Minimum (2031–2060)		
	Annapurna	Langtang	Khumbu	Annapurna	Langtang	Khumbu
DJF	0.0282	0.0279	0.0291	−0.0033	0.0038	0.0128
MAM	0.0235	0.0175	1.1798	0.0531	0.8885	0.9675
JJAS	0.1895	−0.0285	1.2070	0.2500	−0.1545	−0.7023
ON	−0.0051	0.0565	0.2222	−0.0196	−0.0408	−0.9862
Annual	0.0714	0.0234	0.6947	0.0925	−0.0552	−0.1522

discharge has an increasing trend in Khumbu, at rates of 0.7282 m³/s/year (2001–2030) and 0.1208 m³/s/year (2031–2060), compared to other regions.

The CGCM3-projected seasonal minimum discharge trend of A1B scenarios over the period 2001–2060 is shown in Table 4.14. The minimum discharge trends in Annapurna and Khumbu are found to be increased in summer, whereas in Langtang the trend is found to be increased during autumn (ON) and decreased in summer (JJAS) in the period 2001–2030. In Langtang and Khumbu, the minimum discharge trend is increasing during spring (MAM), but during summer (JJAS) in Annapurna, in the period 2031–2060. Similarly, the minimum discharge trends are found to occur in Annapurna and Khumbu, whereas these occur during summer in Langtang (JJAS) (2031–2060). The highest annual minimum discharge trend is found in the Khumbu region at the rate of 0.6947 m³/s/year (2001–2030), whereas it is 0.0925 m³/s/year in the Annapurna region (2031–2060), and the lowest value of −0.1522 m³/s/year, is found in the Khumbu region.

4.6 Discussion

The observed highest annual maximum temperature trend of 0.1414 °C/year is found in the Langtang region, and the lowest minimum temperature trend (−0.0024 °C/year) is observed in the Khumbu region. The GCMS-simulated seasonal and annual range of mean of 20 ensembles for temperature scenarios with

A1B emission scenarios at Annapurna, Langtang, and Khumbu region, and the projected annual maximum and minimum temperature trends ($0.0203\text{ }^{\circ}\text{C}/\text{year}$ and $0.0300\text{ }^{\circ}\text{C}/\text{year}$), are found to be increasing in Langtang compared to Khumbu and Annapurna regions for the period 2031–2060. The observed annual precipitation trends are increasing at the rate of $2.7452\text{ mm}/\text{year}$ and $10.608\text{ mm}/\text{year}$ in Annapurna and Langtang regions, respectively. However, the observed annual precipitation trend has been found decreasing at $-0.8264\text{ mm}/\text{year}$ in the Khumbu region.

The projected annual precipitation trends are found to be increasing at the rate of $2.9232\text{ mm}/\text{year}$ and $1.4753\text{ mm}/\text{year}$ in Annapurna region (2001–2030 and 2031–2060, respectively), although decreasing at $0.7621\text{ mm}/\text{year}$ and $0.2084\text{ mm}/\text{year}$ in Langtang region (2001–2030 and 2031–2060, respectively). Correspondingly, projected annual precipitation has an increasing trend of $1.9991\text{ mm}/\text{year}$ and a decreasing trend of $-0.8264\text{ mm}/\text{year}$ in the Khumbu region for 2001–2030.

The annual observed discharge trends of $-0.2984\text{ m}^3/\text{s}/\text{year}$, $-0.3799\text{ m}^3/\text{s}/\text{year}$, and $2.3072\text{ m}^3/\text{s}/\text{year}$ are found in Annapurna, Langtang, and Khumbu regions, respectively, whereas annual observed discharge has an increasing trend in Khumbu. The projected annual maximum discharge at the rate of $0.0833\text{ m}^3/\text{s}/\text{year}$ and $0.1208\text{ m}^3/\text{s}/\text{year}$ is found in Annapurna region (2001–2030 and 2031–2060, respectively). The projected highest annual maximum discharge trend is found in Langtang region at the rate of $0.0277\text{ m}^3/\text{s}/\text{year}$ and $0.0315\text{ m}^3/\text{s}/\text{year}$ (2001–2030 and 2031–2060, respectively). The projected highest annual maximum discharge trend is found in Khumbu region at the rate of $0.7282\text{ m}^3/\text{s}/\text{year}$ and $0.0193\text{ m}^3/\text{s}/\text{year}$ (2001–2030 and 2031–2060, respectively). Similarly, the highest projected annual minimum discharge trend of $0.0714\text{ m}^3/\text{s}/\text{year}$ and $0.0925\text{ m}^3/\text{s}/\text{year}$ occurs in Annapurna, that of $0.0234\text{ m}^3/\text{s}/\text{year}$ and $-0.0552\text{ m}^3/\text{s}/\text{year}$ in Langtang region, and that of $0.6947\text{ m}^3/\text{s}/\text{year}$ and $-0.0552\text{ m}^3/\text{s}/\text{year}$ in Khumbu region (2001–2030 and 2031–2060, respectively). By using the A1B scenario from the CGCM3 data set and downscaling precipitation and temperature data for discharge projection, the results showed that the downscaled precipitation data are suitable for the study of climate change impact on flow regime in these three glacier-fed basins. The results of observed and simulated discharge obtained from the HVB-*light 3.0* model display a similar pattern when comparing the performance in simulation of historical stream flows in the three river basins.

The overall summary and results of analysis of the seasonal temperature obtained from the A1B scenario of climate projection show that a significant increase in maximum temperature during the spring season is projected, except in the Langtang region, whereas the discharge trend is increasing in summer in Annapurna and Langtang regions. Similarly, minimum temperature is found to have an increasing trend in the spring season in Annapurna and Langtang regions, whereas the minimum discharge is increasing in the subsequent season summer season during 2001–2030, except in Langtang and Khumbu regions, during 2031–2060; this difference could be caused by the melting of snow and the glacier combined with a decrease in rainfall in these regions. Similarly, the seasonal analysis of the precipitation data shows precipitation trends to increase significantly during the spring season in most

cases but the flow regime (discharge) is more pronounced in the subsequent season, that is, in summer; this finding results from the good response of the discharge scenario for temperature and precipitation.

4.7 Conclusion

The performance of SDSM downscaling, based on GCM predictors at three basins, was evaluated using the statistical properties of daily climate data. It is found that the application of SDSM for statistical downscaling is suitable for developing daily climate scenarios. To demonstrate the procedure of developing such scenarios, SDSM is applied based on the daily outputs of common climate variables from GCM simulations, which have been widely used in the development of daily climate scenarios; the results can be used in many areas of climate change impact studies. Based on the analysis of results, CGCM3 model has been found to be a useful model for the simulation of future temperature and precipitation scenario.

Both the annual (maximum and minimum) temperature trends of the A1B scenario in all three regions are found to have increasing trends for the periods of 2001–2030 and 2031–2060. The distribution of precipitation is controlled by the orientation of the mountain systems. This effect causes the middle mountain and windward side to receive relatively more precipitation than the high mountain, valley, and leeward side. Observed annual precipitation is increasing in Annapurna and Langtang regions, whereas no such trend is found in the Khumbu region. The annual precipitation of the A1B scenario of all three regions is increasing in both periods, 2001–2030 and 2031–2060, except in the Khumbu region for 2031–2060.

The annual maximum discharges of the A1B scenario of three basins are increasing during both periods, 2001–2030 and 2031–2060, as a consequence of monsoon rainfall responses. The minimum discharge scenario is increasing only in the Annapurna region, but a decreasing trend is found in the Langtang and Khumbu regions for the period 2031–2060. The flow regime (discharge) trend is more pronounced after the subsequent summer (JJAS) season during both the 2001–2030 and 2031–2060 time periods.

Acknowledgments The authors thank Dr. Rishi Ram Sharma, the director general, and Mr. Suresh Chand Pradhan, hydrologist, of the Department of Hydrology and Meteorology (DHM), Government of Nepal, for providing the necessary data for this research. We heartily acknowledge Dr. Jan Seibert and the Uppsala University's Department of Earth Hydrology for supporting the software HBV-Light 3.0. We are grateful to the Data Access Integration (DAI, see <http://quebec.ccsn.ca/DAI/>) Team for providing the data and technical support. The DAI data download gateway is a collaboration among the Global Environmental and Climate Change Centre (GEC3), the Adaptation and Impacts Research Division (AIRD) of Environment Canada, and the Drought Research Initiative (DRI).

References

- Allen RG, Pereira L, Raes D, Smith M (1998) Crop evapo-transpiration: guidelines for computing crop water requirements. FAO Irrigation and Drainage Paper 56. FAO, Rome, p 17
- Bergstrom S (1992) The HBV model its structure and applications. SMHI Reports Hydrology, No. 4. Norkioping, Sweden: 32
- Bergstrom S, Graham LP (1998) The Baltic basin – a focus for interdisciplinary research. Nordic Hydrological Conference, Aug 11–12, Helsinki
- Charlton R, Fealy R, Moore S, Sweeney J, Murphy C (2006) Assessing the impact of climate change on water supply and flood hazard in Ireland using statistical downscaling and hydrological modeling techniques. *Clim Change* 74:475–491
- Gordon C, Cooper C, Senior CA, Banks H, Gregory JM, Johns TC, Mitchell JFB, Wood RA (2000) The simulation of SST, sea ice extents and ocean heat transport in a version of the Hadley Centre coupled model without flux adjustments. *Clim Dyn* 16:147–168
- Konz M, Merz J (2010) An application of the HBV model to the Tamor basin in Eastern Nepal. *J Hydrol* 7:49–58
- Mahmood R, Mukand BS (2012) Evaluation of SDSM developed by annual and monthly submodels for downscaling temperature and precipitation in the Jhelum basin, Pakistan and India. *Theor Appl Climatol* 113:27–44
- Manley RE (1993) HYSIM reference manual. RE Manley Consultancy, Cambridge
- Murphy C, Charlton R, Sweeney J, Fealy R (2006a) Catering for uncertainty in a conceptual rainfall runoff model: model preparation for climate change impact assessment and the application of GLUE using Latin Hypercube Sampling. In: Proceedings of the National Hydrology Seminar, Tullamore, 2006
- Raghunath HM (2006) Hydrology, principles, analysis and design. New Age International (P) Limited, New Delhi
- Rashid M, Mukand BS (2012) Evaluation of SDSM developed by annual and monthly sub-models for downscaling temperature and precipitation in the Jhelum basin, Pakistan and India.
- Salzmann N, Frei C, Vidale P, Hoelzle M (2007) The application of regional climate model output for the simulation of high-mountain permafrost scenarios. *Global Planet Change* 56:188–202
- Seibert J (2005) HBV light version 2, user's manual. Institute of Earth Sciences, Department of Hydrology, Uppsala University, Uppsala
- Sen PK (1968) Estimates of the regression coefficient based on Kendall's tau. *J Am Stat Assoc* 63:1379–1389
- Silveira L (1997) Multivariate analysis in hydrology: the factor correspondence analysis method applied to annual rainfall data. *Hydrol Sci* 42(2):215–224
- Wang H (2006) Inter-annual and seasonal variation of the Huang He (Yellow River) water discharge over the past 50 years: connection to impacts from ENSO events and dams. *Global Planet Change* 50:212–225
- WMO (1988) Analyzing long time series of hydrological data with respect to climate variability. Project description. WCAP-3. Technical Report, World Meteorological Organization, Geneva